ACI JOURNAL TECHNICAL PAPER

Title no. 82-4

Basic Tools of Reinforced Concrete Beam Design

by Peter Marti

The application of consistent equilibrium and ultimate strength considerations to the design and detailing of reinforced concrete beams is described. Basic tools include struts and ties, nodes, fans, and arches. Comparisons with experiments on a shearwall coupling beam and on a deep beam, and three design examples illustrate the practical application of these tools.

Keywords: beams (supports); deep beams; **detailing;** girders; limit design method; plastic analysis; **reinforced concrete;** shear strength; shearwalls; **strength; structural design.**

During the past two decades much work has been done in the field of limit analysis and design of reinforced concrete.[1-4] Particularly useful results have been obtained regarding (1) the strength of slabs and (2) the strength of beams under shear, torsion, and combined actions. Rational models have been proposed which are adequately accurate and sufficiently simple and general for practical applications. These developments had a big influence on the formulation of European codes.[5-7] In North America, similar proposals for shear and torsion design found wide attention in recent years.[8]

Considering the behavior of the concrete, the application of limit analysis methods to reinforced concrete is questionable. However, the majority of all reinforced concrete members are under-reinforced. Their strength is essentially determined by the yield strength of the reinforcement. The concrete model does not have a pronounced influence. In addition, detailed comparisons with experiments revealed that limit analysis approaches lead to quite satisfactory strength predictions even for over-reinforced cases if an appropriate effective concrete compressive strength is taken into account.

The limit analysis approaches can be subdivided into static (lower-bound) and kinematic (upper-bound) methods. While a kinematic approach is generally best suited for analyzing an existing design, the static method is directly applicable in design and detailing because it provides a possible equilibrium system of internal forces throughout a structure under ultimate loads and thus it indicates the required strengths of both concrete and reinforcement.

Limit analysis and design of reinforced concrete slabs is well known.[1,9-11] Similarly, the application of the upper-bound method to reinforced concrete beams has been treated extensively.[1,2,12] However, the systematic application of the lower-bound approach to the design of reinforced concrete beams is not yet well known. It is the purpose of this paper to summarize and to extend some of the existing work in this area.[3,12-15] It will be shown that it is possible to consider equilibrium solutions to rather complex problems in a simple way.

The suggested design procedure consists of three steps. Based on experience, the designer first chooses initial concrete dimensions which are deemed to allow normal construction and to satisfy the serviceability and ultimate strength requirements. In a second step, the concrete dimensions and the dimensions, the distribution, and the details of the reinforcement are determined on the basis of consistent equilibrium and ultimate strength considerations. Limits for the amount and the distribution of the reinforcement are observed to insure the required redistribution of the internal forces in the cracked state. If necessary, additional kinematic considerations are made in a third step to check the behavior under service conditions and to further investigate the redistribution of the internal forces when approaching failure.

Similar to the end product of their application, the design drawings, the basic tools used in step two of the suggested design procedure are by nature geometrical. Truss models are used to investigate the equilibrium between the loads, the reactions, and the internal forces in the concrete and in the reinforcement. Statically admissible stress fields are developed by replacing the truss members by struts and ties, fans, and arches with finite dimensions. The pin connections of the trusses correspond to biaxially or triaxially stressed nodal zones.

This paper describes these basic tools and illustrates their application to typical design problems. The presentation is restricted to plane problems. Some exten-

Received July 28, 1983, and reviewed under Institute publication policies.

ACI member **Peter Marti** *is an associate professor of structural engineering at the University of Toronto, Toronto, Canada. Dr. Marti is a member of ACI-ASCE Committee 421, Design of Reinforced Concrete Slabs; ACI-ASCE Committee 445, Shear and Torsion; CEB Commission IV, Members Design; and the Canadian Code Committee CSA N287, Concrete Containment Structures for Nuclear Power Plants.*

sions to three-dimensional problems are given elsewhere.[3,14,15]

STRUT AND TIE ACTION

The single load V acting on the deep beam shown in Fig. 1(a) is transferred to the support BC over the inclined strut ACDF. The horizontal and vertical components of the strut force are $T = C = \omega htf_c$ and $V = \omega(1-\omega)h^2tf_c/a$, respectively, where f_c denotes the effective concrete compressive strength and ω is the mechanical reinforcement ratio corresponding to the longitudinal reinforcement whose center is at a distance of $\omega h/2$ from the bottom of the beam. The triangular zones ABC and DEF are biaxially compressed to $-f_c$.

Since the concrete tensile strength is neglected and the beam is only longitudinally reinforced, no bond forces can be developed in the shear span a. Therefore, the reinforcement must be fully anchored behind the support. Fig. 1(a) shows a possible solution with an end plate AB. Another possibility is to use hairpin-shaped reinforcing bars as shown in Fig. 1(b). The force transfer from the hairpins to the concrete is somewhat similar to the situation at the bottom of stirrup-reinforced T-beams.[15] Compressed shells spanning between the bends of the hairpins may distribute the force T onto the concrete which is enclosed by the hairpins. To improve the support of these shells, it is advantageous to place strong vertical dowel bars in the bends of the hairpins. While the described shell action requires only compression in the concrete, tensile stresses are necessary across the vertical planes defined by the legs of the hairpins to activate the concrete cover.

The discontinuous stress field represented in Fig. 1(a) is a highly idealized model of the stress state at ultimate. In reality, the concrete tensile strength and bond forces are mobilized under increasing load to achieve as stiff a response as possible. Cracking indicates the successive development of new static systems and the bond may gradually deteriorate. Eventually, the load may be carried by strut and tie action.

Strut and tie action was apparently first discussed by Moersch.[16] Drucker[17] introduced discontinuous stress fields similar to Fig. 1(a). Subsequently, the kinematics of the problem was investigated assuming that the strength of concrete in plane stress is governed by a no-tension and a no-crushing criterion and that the associated flow rule is valid.[2,12,14] The most general failure mechanisms which are compatible with the stress field of Fig. 1(a) involve a hyperbolic failure surface[12] through Points C and F and a relative rotation of the separated parts of the beam about a point lying on one of the two extensions of the strut diagonal AD.[14] Using coordinate axes x and y aligned with the strut direction and with origin at the center of rotation, the equation of all possible failure surfaces is xy = constant. To facilitate comparisons with experiments, these considerations were extended to treat the influence of an arbitrary position of the longitudinal reinforcement and to discuss the effect of an overhang behind the support as well as the influence of the length of the support and load plates.[18]

Strut and tie models are directly applicable in design. After having chosen a suitable value f_c, the required size, position, distribution, and anchorage of the main reinforcement can be determined. This is best done by drawing to scale an assumed truss, determining the required strut widths, and modifying the truss geometry if necessary. Technological constraints given by bend diameters of reinforcing bars, concrete cover, etc., can easily be taken into account. Some typical applications are represented in Fig. 1(c) through (f). In every case, it is of decisive importance to insure with careful and consequent detailing that the truss forces can be devel-

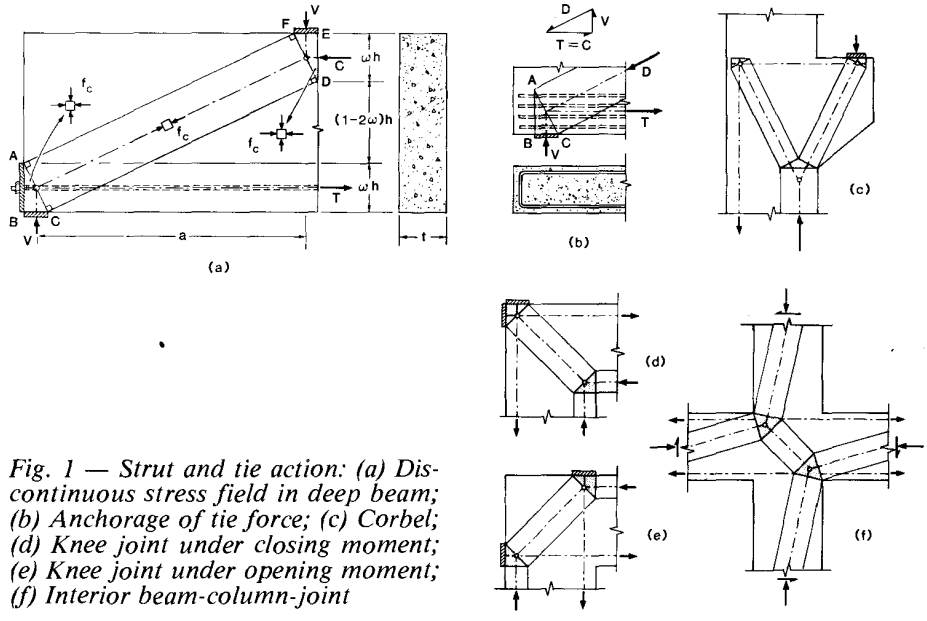

Fig. 1 — Strut and tie action: (a) Discontinuous stress field in deep beam; (b) Anchorage of tie force; (c) Corbel; (d) Knee joint under closing moment; (e) Knee joint under opening moment; (f) Interior beam-column-joint

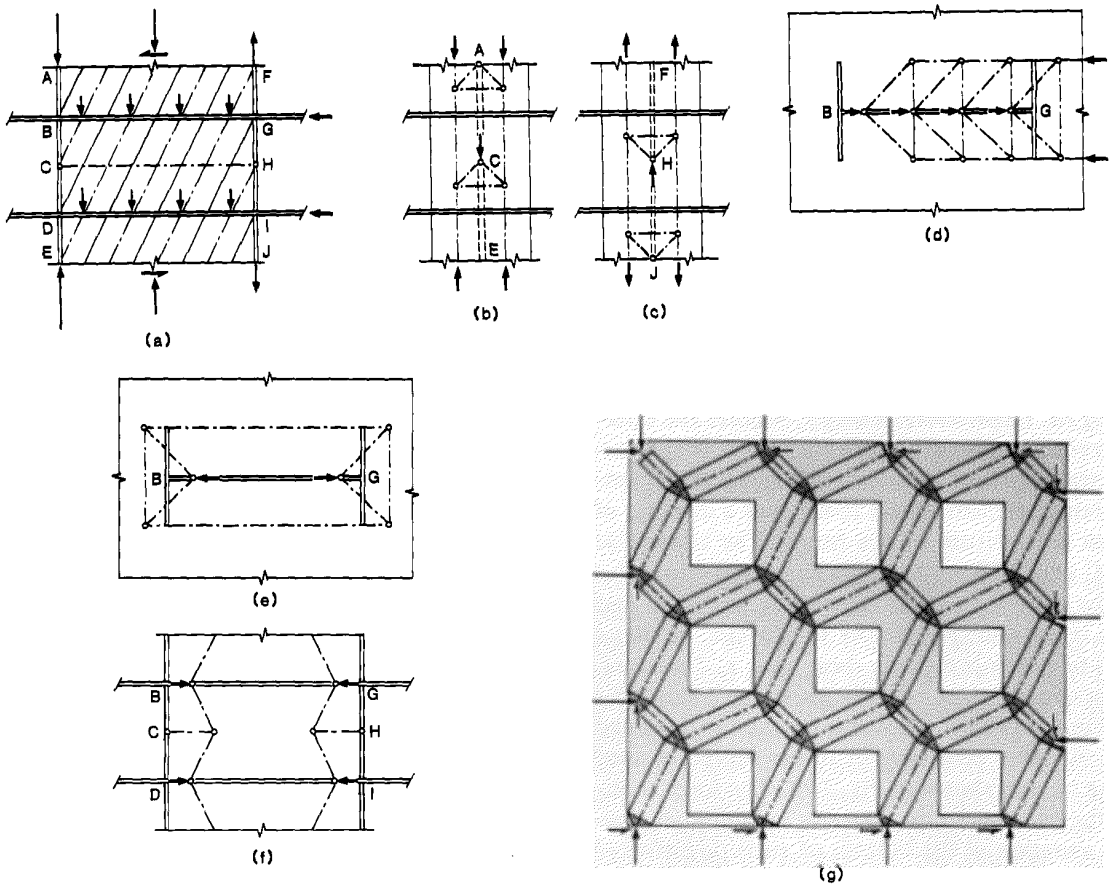

Fig. 2 — Strut and tie action in shearwalls: (a) Truss model of web of I-shaped wall; (b) Truss model of compression flange; (c) Truss model of tension flange; (d) Truss model of force transfer in floor slab; (e) Truss model of floor slab acting as external stirrup of web; (f) Truss model showing effect of external stirrup action on web; (g) Strut action in shearwall with openings

oped and transferred at the required locations. Failure to meet this requirement inevitably leads to reduced capacities.

Comparisons with experiments indicate a reasonable first choice of f_c is 60 percent of f'_c . This value may be decreased or increased depending on the specific circumstances such as required redistribution of internal forces, presence of distributed reinforcement, presence of lateral confinement, etc. Members with low reinforcement ratios are rather insensitive to the assessment of f_c. However, a cautious approach is recommended for members with intermediate and high reinforcement ratios. Some guidance is obtained by comparing the suggested value $f_c = 0.6f'_c$ with the stress limits of $0.85f'_c$ for flexure and axial load, $0.67f'_c$ for shear (assuming effective depth in shear to be 90 percent of effective depth in flexure) and $0.5f'_c$ for torsion according to Clauses 10.4.3.2, 11.2, and 12.3.2 of the CEB-FIP model code,[6] respectively. Note that for members in shear and torsion the CEB-FIP model code limits the angle between the principal compressive stress trajectories in the concrete and the member axis by $\tan^{-1}$ (3/5) and $\tan^{-1}$ (5/3); i.e., it restricts the reorientation of the principal compressive stress direction in the concrete after cracking to a range of ± 14 deg. Rather than giving a constant value f_c/f'_c and restricting the inclination of the diagonal compression fields, Collins and Mitchell[8] consider the strains associated with uniform diagnoal compression fields and express f_c/f'_c as a function of the ratio of the principal strains. Adaptation of this refined approach to nonuniform stress fields is possible. This leads to realistic estimates of f_c and limits effectively the amount of reinforcement that can be taken into account for ultimate strength.

In deep beam design, a distributed minimum reinforcement corresponding to geometrical reinforcement ratios of about 0.2 to 0.6 percent is usually provided. Apart from its beneficial effect on the cracking behavior, this reinforcement contributes significantly to the ability of a deep beam to redistribute the internal forces after cracking. While from a strength point of view the distributed vertical reinforcement essentially allows curtailment of the longitudinal reinforcement, the contribution of the distributed longitudinal reinforcement to the strength is sometimes of such a magnitude that it should be taken into account when designing the main longitudinal reinforcement.[13]

As a further illustration of the transparency and adaptability of truss models, consider an I-shaped shearwall (Fig. 2). Fig. 2(a) shows a series of inclined struts making up a compression field in the web AEJF. Equilibrium of the horizontal forces along the web-

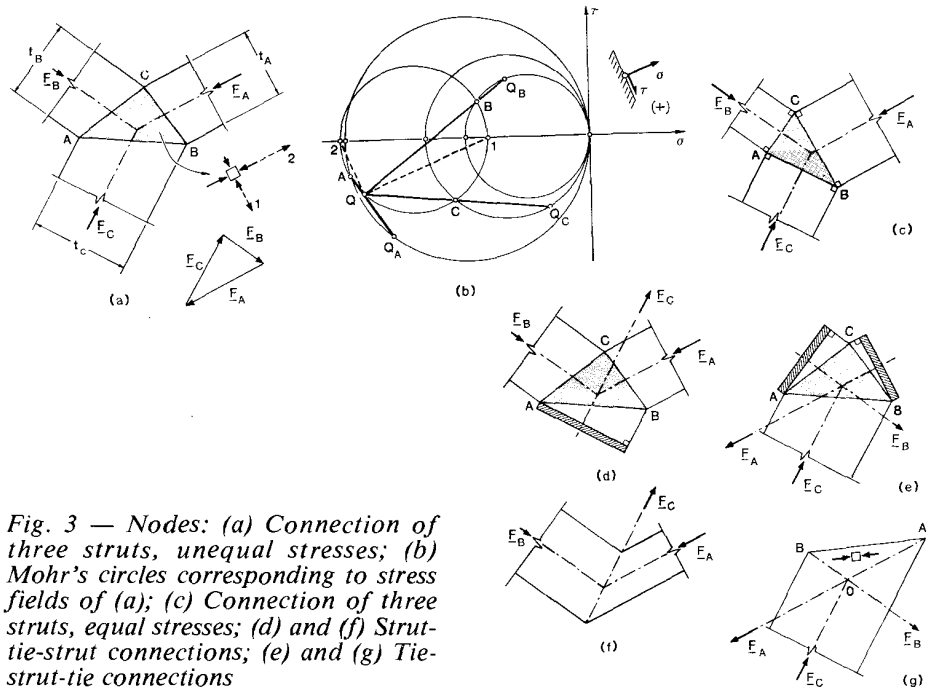

Fig. 3 — Nodes: (a) Connection of three struts, unequal stresses; (b) Mohr's circles corresponding to stress fields of (a); (c) Connection of three struts, equal stresses; (d) and (f) Strut-tie-strut connections; (e) and (g) Tie-strut-tie connections

flange connections BD and GI requires a uniformly distributed horizontal web reinforcement whose strength is given by the force in truss member CH. The necessary transverse flange reinforcement can be determined using truss models as shown in Fig. 2(b) and (c). Fig. 2(d) shows a model for the transfer of horizontal forces through a floor slab to the web of the shearwall. The floor slabs may also provide an external stirrup effect on the shearwalls. This is illustrated in Fig. 2(e) and (f). Rather than transferring the horizontal force components of the inclined compression field from one side of the web to the other as shown in Fig. 2(a), these forces may be transferred to the adjoining floor slabs and equilibrated by them. Finally, Fig. 2(g) shows a possible strut action in a shearwall with openings.

NODES

Fig. 3(a) shows an equilibrium system of three strut forces. When strut widths are chosen, three different uniaxial compressive stress fields are created. The intersection points A, B, and C of the strut edges define a biaxially stressed triangular zone. The stress state in this zone is found by drawing parallel lines to the sides BC, CA, and AB of the triangle through the poles Q_A, Q_B, and Q_C of the individual struts' Mohr's circles in Fig. 3(b). The intersection points A, B, and C of these lines with the corresponding Mohr's circles define the Mohr's circle for the biaxial compressive stress state in the triangle ABC of Fig. 3(a). The center of this circle must lie on the σ-axis and the straight lines Q_AA, Q_BB, and Q_CC must all intersect in its pole Q.

If the strut widths are chosen so that the stresses in all struts are equal to $-\sigma$, the principal stresses in the triangular nodal zone are $\sigma_1 = \sigma_2 = -\sigma$ and the sides of the triangle are perpendicular to the struts, see Fig. 3(c). This result has already been used in Fig. 1 and 2(g).

Fig. 3(d) and (e) illustrate how tie forces can be converted to compressive forces acting from behind on the nodal zone using end plates or similar solutions.

Fig. 3(f) and (g) show alternatives in which tie forces are developed over bond. The choice of one strut width determines the width of the second strut in Fig. 3(f). The choice of the strut width in Fig. 3(g) determines the points A and B. In the triangle OAB a uniaxial compressive stress field parallel to the line AB is developed. Bond forces are acting along OA and OB. It should be emphasized that nodal zones corresponding to Fig. 3(f) and (g) require a proper lateral confinement. The finite spacing of the reinforcing bars causes a local deviation from a plane stress problem which may be treated using similar concepts as for the anchorage problem of hairpins above, i.e., compressed shells spanning between the single reinforcing bars. The main function of the lateral confinement is to provide sufficient lateral support of these shells.

FAN ACTION

Consider a uniformly loaded deep beam having a length of $2a$. In Fig. 4(a) the load qa acting on one-half of the beam is replaced by two statically equivalent single loads $qa/2$. These loads are transferred to the support BC by the struts ADEG and DCHK. The thickness of the compression zone EKJF is $\omega h/4$, the lengths of the plates AB and BC are ωh and $qa/(tf_c)$, respectively, and the nodal zones ABCD, EFG, and HIJK are all biaxially compressed to $-f_c$. The force $T = C$ is equal to ωhtf_c and ω is given by $2\omega(1 - \omega)h^2tf_c = qa^2[1 - q/(tf_c)]$.

Going back to the original problem, the fan-shaped stress field ACDF shown in Fig. 4(b) is obtained by subdividing the length EF into differential elements dx and considering elementary struts carrying loads qdx. The lines AC and FD are quadratic parabolas.[14] The

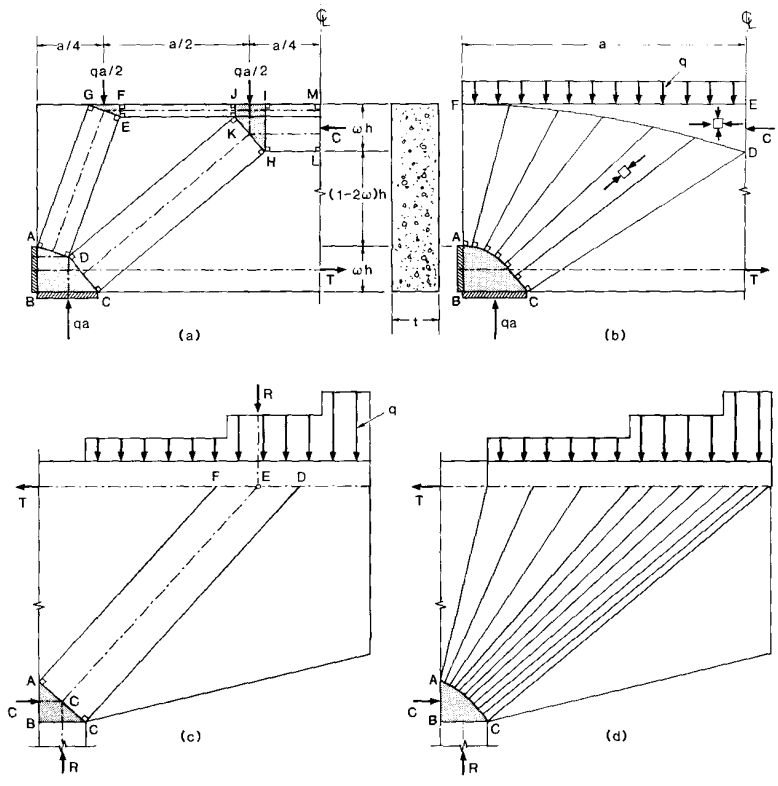

Fig. 4 — Fan action: (a) Strut and tie model of uniformly loaded deep beam; (b) Fan-shaped stress field; (c) Strut and tie system for equivalent single load R *replacing distributed load q; (d) Continuous fan developed from discrete strut*

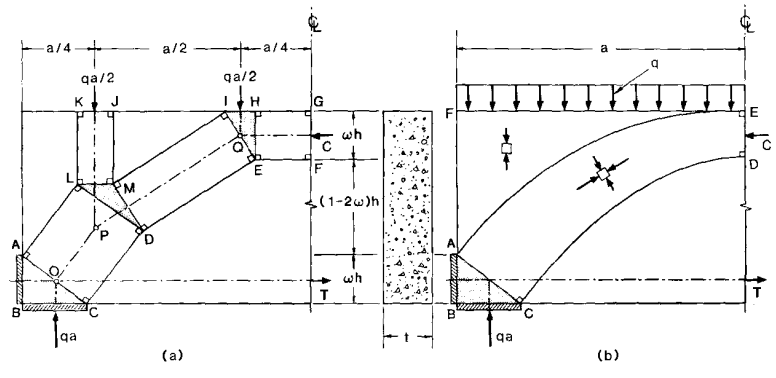

Fig. 5 — Arch action: (a) Strut and tie model; (b) Continuous arch

points A, C, and D coincide with points A, C, and L of Fig. 4(a), respectively. Along their straight trajectories the principal compressive stresses in the fan region vary hyperbolically.[12,14] The principal stresses in the compression zone DEF are $\sigma_1 = -q/t$ and $\sigma_2 = -f_c$.

Fan-shaped stress fields can easily be developed for arbitrary loads. The distributed load acting on the cantilever of Fig. 4(c) is replaced by the statically equivalent single load R. Load R is carried by the inclined strut ACDF and the horizontal force $T = C$. Equilibrium determines the location of the pin connection E of the imaginary truss and the choice of f_c determines the second pin connection O. Going back to the original problem means replacing the discrete strut by a continuous fan [see Fig. 4(d)]. The line AC is now curved but Point A coincides with Point A of Fig. 4(c).

ARCH ACTION

Fig. 5(a) and (b) show alternative stress fields for the problems of Fig. 4(a) and (b). The thickness of the flexural compression zone at midspan as well as the lengths of the plates AB and BC are the same in all cases. The strut system of Fig. 5(a) is a discrete model of the continuous arch ACDE shown in Fig. 5(b). The boundary lines DC and EA of this arch are quadratic parabolas. The trajectories of the principal stresses σ_1 in the arch are straight lines perpendicular to the parabola DC and the principal stresses in the arch are $0 \geqslant \sigma_1 \geqslant -q/t$ and $\sigma_2 = -f_c$.[14]

COMBINED STRUT AND FAN ACTION

Fig. 6(a) shows the dimensions of Paulay's shearwall coupling beam No. 391.[19] This beam was monotoni-

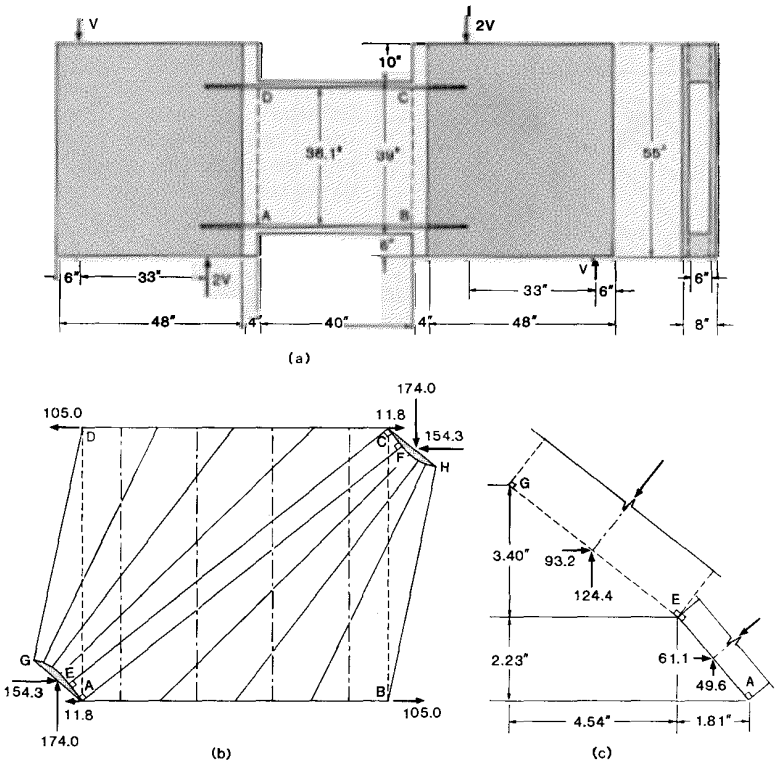

Fig. 6 — Combined strut and fan action: (a) Geometry and loading of Paulay's[19] shearwall coupling beam No. 391 (1 in. = 25.4 mm); (b) Stress field and forces (1 kip = 4.45 kN); (c) Detail of nodal zone AEG

cally loaded to failure. The concrete compressive strength per unit length of the 6 in. (152 mm) thick central test region was 27.4 kips/in. (4798 kN/m) and the yield strength of the distributed vertical stirrup reinforcement was 3.11 kips/in. (545 kN/m). The yield strengths of the concentrated longitudinal reinforcements along AB and CD were 105 kips (467 kN) and that of an additional distributed longitudinal reinforcement was 37.4 kips (166 kN).

Using the given values the stress field of Fig. 6(b) can be developed. The theoretical ultimate load V = 174 kips (774 kN) is partly carried by the strut AFCE [V_s = 49.6 kips (221 kN)] and partly by the yielding stirrups and the two fans ECDG and ABHF [V_f = 124.4 kips (553 kN)]. The distributed longitudinal reinforcement yields throughout the test region and the forces in the concentrated longitudinal reinforcements decrease along BA and DC due to the fan action from 105 kips (467 kN) to 11.8 kips (52 kN).

For the development of Fig. 6(b) the stirrup reinforcement and the fans are replaced by a statically equivalent single stirrup at midspan and by single struts, respectively. Starting from an assumed value V_s, the points E and F are geometrically determined. Since V_f is known, the centers of the lines EG and FH and the points G and H are then also found geometrically. Cutting the test region along its diagonal BD and formulating equilibrium of the horizontal forces reveals that the sum of the horizontal force components in the strut AFCE and in the two fans must be equal to 2 × 105 + 37.4 = 247.4 kips (2 × 467 + 166 = 1100 kN). This requirement can be used to correct the initial assumption on V_s. After a few iterations the details shown in Fig. 6(c) result. Note that 2 × 93.2 + 61.1 = 247.5 kips (2 × 415 + 272 = 1102 kN). An extension of the presented stress field beyond the biaxially compressed nodal zones AEG and CFH into the 8 in. (203 mm) thick end blocks is given elsewhere.[18]

The experimental ultimate load was 174.5 kips (776 kN). Stirrups and longitudinal reinforcement yielded and the concrete was crushed. The crack pattern resembled the picture of the principal compressive stress trajectories given in Fig. 6(b).

COMBINED ARCH AND FAN ACTION

To investigate the effect of stirrups on the strength of deep beams the strut and tie model of Fig. 7(a) is analyzed. One part of the load V is transferred over the strut NKPQ and a single stirrup to GH. There it adds to the force in strut FKJH which carries the remainder of V. The depths AB and LO are equal. The forces in the longitudinal reinforcement at points D and I are proportional to LO and LN, respectively. Thus, in comparison with a deep beam without stirrups, the lever arm of the internal forces $C = T$ is increased by one-half of the depth NO.

In Fig. 7(b) the discrete strut and tie model of Fig. 7(a) is replaced by a combination of an arch EFKJ and a fan DINK. The points A through E and I through O in both figures coincide. In Fig. 7(b) the variation of the force in the longitudinal reinforcement is indicated. Apart from the slight increase of the lever arm of the internal forces, the addition of stirrups also allows curtailment of the longitudinal reinforcement. It should be

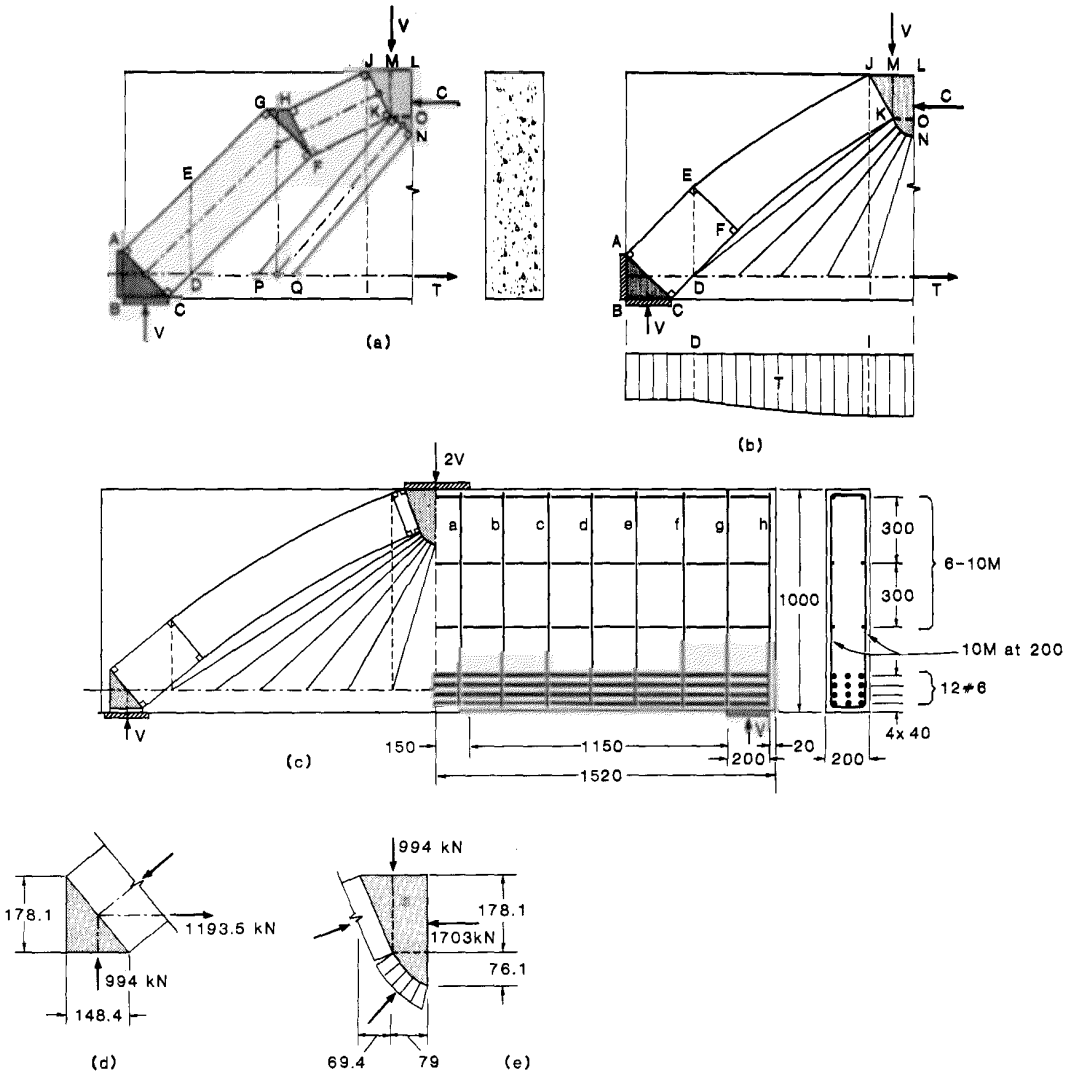

Fig. 7 — Combined arch and fan action: (a) Strut and tie model; (b) Stress field and variation of force in longitudinal reinforcement; (c) Geometry and loading of Lee's[20] beam No. SD-1 (right) (1000 mm = 39.4 in.), and stress field (left); (d) Nodal zone above support (1 kN = 0.225 kip); (e) Nodal zone below load

emphasized, however, that in any case a substantial portion of the longitudinal reinforcement must be anchored behind the support.

Fig. 7(c) shows the application of the model of Fig. 7(b) to Lee's test beam No. SD-1.[20] The dimensions and the reinforcement are given in Fig. 7(c). The cross-sectional area of one 10 M bar is equal to 100 mm^2 (0.155 in.^{2}). The yield strength of the 10 M bars was 529 MPa (76.7 ksi) and that of the #6 bars was 498 MPa (72.2 ksi). Compressive strength f'_c was 33.5 MPa (4860 psi) and the concrete cover was 15 mm (0.59 in.).

In developing the stress field shown in Fig. 7(c), it was assumed that Stirrups b through f as well as the main horizontal reinforcement at midspan yielded. The influence of the six longitudinal 10 M bars was neglected. Fig. 7(d) and (e) show details of the stress field which were found after an iterative procedure similar to the one applied to the shearwall coupling beam. The yielding stirrups carry 529 kN (118.9 kips) of the theoretical ultimate load V = 994 kN (223.5 kips). The force in the longitudinal reinforcement is reduced from its yield strength 1703 kN (382.9 kips) at midspan to 1193.5 kN (268.3 kips) at the support.

The actual failure occurred at a load V = 967.5 kN (217.5 kips) by sudden crushing of one support region followed by loss of anchorage of the longitudinal reinforcement. Large pieces of the concrete cover spalled off and large transverse splitting cracks developed extending from the crushed region upward. Prior to failure, the average strains in the longitudinal reinforcement just reached the yield limit between Stirrups a and b and decreased to about 70 percent of this value between Stirrups f and g. Yielding was also observed in Stirrups e, f, and h. The strains in Stirrups c and d were not measured but certainly they reached the yield limit. Finally, the maximum average strains observed in Stirrups b and g were about 0.002. It is remarkable that the beam was able to carry such a high load although the #6 bars were straight, i.e., no special anchorage was provided. Obviously, some lateral confinement was

Fig. 8 (right)—Design example 1: (a) Geometry and loading (1000 mm = 39.4 in., 1 kN = 0.225 kip); (b) Truss model of web; (c) Stress field in web; (d) Required and provided bottom reinforcement; (e) Required and provided top reinforcement; (f) Required and provided web stirrups; (g) Truss model and transverse reinforcement of top flange; (h) Required and provided transverse reinforcement of bottom flange; (i) Cross sections

provided by Stirrups g and h, by friction between the support plate and the beam, and by the #2 transverse bars which were used to support the #6 bars.

DESIGN EXAMPLE 1

The reinforcement of the I-beam of Fig. 8(a) will be designed for the given ultimate loads assuming a yield strength of the reinforcement f_y = 400 MPa (58 ksi) and an effective concrete compressive strength f_c = 30 MPa (4350 psi). Fig. 8(b) shows a truss model of the web. The chords of the truss coincide with the flange centers, i.e., the effective web height is equal to 750 mm (29.5 in.). For the inclination of the truss diagonals between the supports the lower limit tan $^{-1}$0.6 suggested by the CEB-FIP model code[6] is used. Therefore, the span of 7500 mm (295 in.) is subdivided into six portions of 750/0.6 = 1250 mm (29.5/0.6 = 49.2 in.), each being subjected to a uniformly distributed load of 225 kN (50.6 kips). In the overhang a 45 deg truss model is used.

Fig 8(c) shows a discontinuous stress field corresponding to the truss model of Fig. 8(b). The triangle BCO is theoretically stress free. Instead of the fans APQ and GHI, parabolic arches could also be used. The fans are centered in the points A, F, and I. In these points the concrete compressive stresses would go to infinity. Taking the finite dimensions of the support and load plates into account would lead to noncentered fans with finite stresses.

In Fig. 8(d) and (e) the variation of the bottom and top flange forces and the chosen longitudinal reinforcements are represented. Fig 8(f) shows the required and provided vertical stirrup reinforcement.

The transverse reinforcement of the top flange is determined using the truss model of Fig. 8(g). The truss diagonals are assumed to form angles of 45 deg. with the beam axis. The required and provided transverse stirrup reinforcement is given in Fig. 8(g). Fig. 8(h) shows the result of a similar consideration for the bottom flange.

In Fig. 8(i) two typical cross sections are represented.

In continuous beams the supports and the points of zero shear force subdivide the webs into regions of similar direction of the inclined compression fields. Once the support reactions have been determined truss models similar to Fig. 8(b) can be developed for arbitrary loads. In Fig. 8(c) the point of zero shear force, O, is just met by the boundaries of the regions ABOP and CDNO. Usually, the stress fields on either side of the points of zero shear force must be terminated by fans.

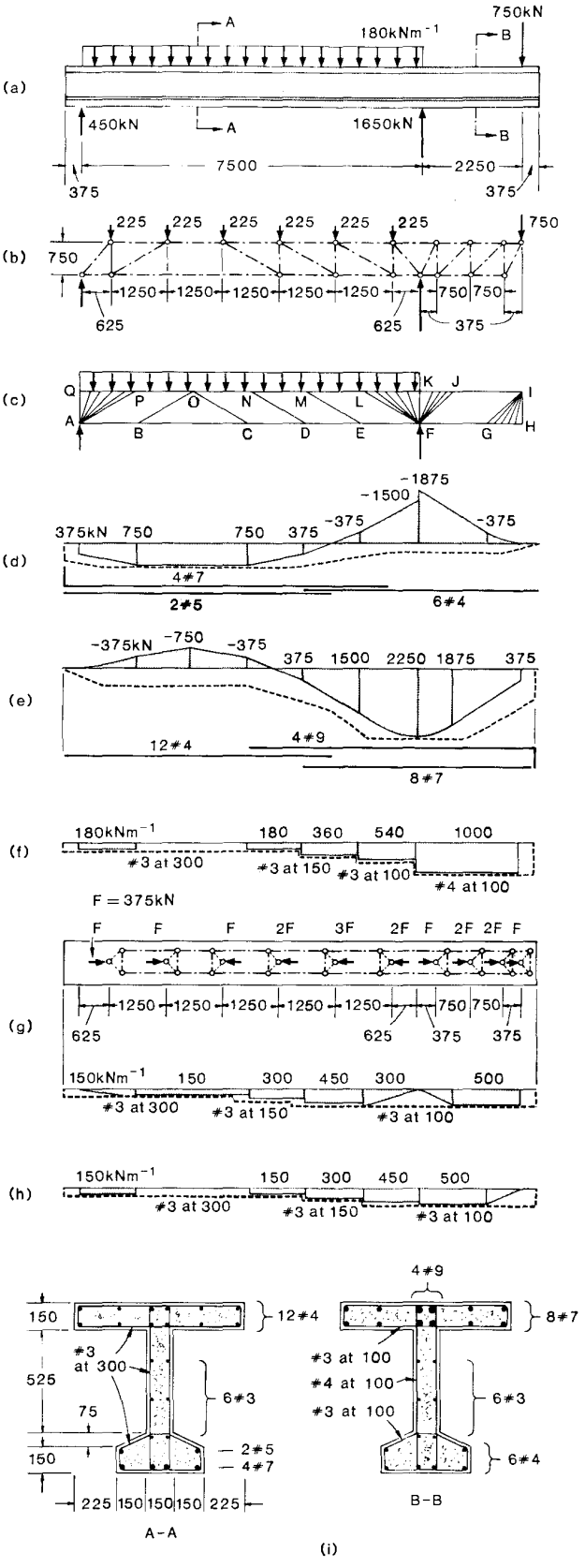

Knowing the forces in the truss diagonals and the widths of the corresponding stress fields, the principal concrete compressive stresses can be calculated. For example, the values -13.6 MPa (-1970 psi) and -13.3 MPa

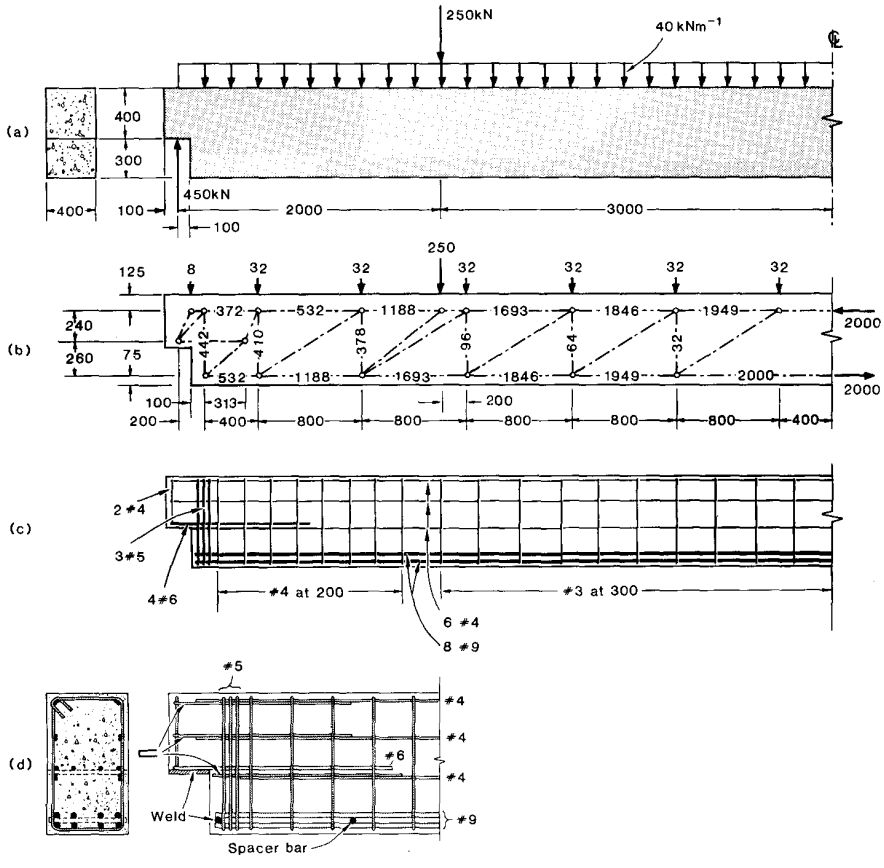

Fig. 9 — Design example 2: (a) Geometry and loading (1000 mm = 39.4 in., 1 kN = 0.225 kip); (b) Truss model; (c) Reinforcement; (d) Detail of draped end

(-1930 psi) are obtained for the regions EFLM and FGIJ of Fig. 8(c), respectively.

It is outside the scope of this paper to discuss the stress states in the web-flange connections and in the flanges in detail. Most critical are the conditions in the vicinity of Point F of Fig. 8(c). Since the bottom flange is almost fully utilized by the compressive forces of 1500 kN (337 kips) and 1875 kN (422 kips), and the additional forces of the fans FKL and FJK cannot easily be spread out in the flange, the effective web height is locally smaller than 750 mm (29.5 in.). Depending on the dimensions of the support plate, this will affect the resultant fan forces and the necessary longitudinal reinforcement. Similar remarks apply to intermediate supports of continuous beams.

DESIGN EXAMPLE 2

The reinforcement of the beam with dapped ends shown in Fig. 9(a) will be designed for the given ultimate loads assuming f_y = 400 MPa (58 ksi), f_c = 20 MPa (2900 psi), and a cover of 20 mm (0.8 in.).

The bending moment of 1000 kN·m (738 ft-kips) at midspan requires a compression zone depth of about 250 mm (9.84 in.) and a reinforcement whose center is about 75 mm (2.95 in.) above the bottom of the beam. Therefore, the truss model with parallel chords shown in Fig. 9(b) is chosen. Towards the supports this model is somewhat conservative because the flexural compression zone depth decreases. The assumed inclination $\tan^{-1}0.625$ of the truss diagonals determines the position of the vertical truss members and also the single loads replacing the uniformly distributed load. The truss geometry in the support region is determined considering the possible placing of the reinforcement.

Fig. 9(c) and (d) show the reinforcement provided to carry the forces given in Fig. 9(b). The strength of the four horizontal #6 bars is 456 kN > 372 kN (102.5 kips > 83.6 kips) and that of the three #5 stirrups is 475 kN > 442 kN (106.8 kips > 99.4 kips). Four #4 stirrups over a length of 800 mm (31.5 in.) take 405 kN (91.1 kips) which is approximately equal to the required 410 kN (92.2 kips) and 378 kN (85.0 kips). The strength of the eight #9 bars is 2052 kN > 2000 kN (461 kips > 450 kips). For four of them a mechanical anchorage is provided. The #3 stirrups and the horizontal #4 bars are a minimum distributed reinforcement.

DESIGN EXAMPLE 3

The shape of the bottom surface of the bridge girder represented in Fig. 10(a) is given by the equation $z = 2\text{ m} + 4\text{ m} \times (x/50\text{ m})^{1.5}$ [$z = 6.56\text{ ft} + 13.12\text{ ft} \times (x/164\text{ ft})^{1.5}$]. The bottom flange thickness decreases linearly from 1.00 m (39.4 in.) at the support to 0.20 m (7.9 in.) at midspan. The average top flange thickness is 0.40 m (15.7 in.), see Fig. 10(b). Therefore, the effective web height decreases from 5.30 m (17.39 ft) to 1.70 m (5.58 ft) as shown in Fig. 10(c).

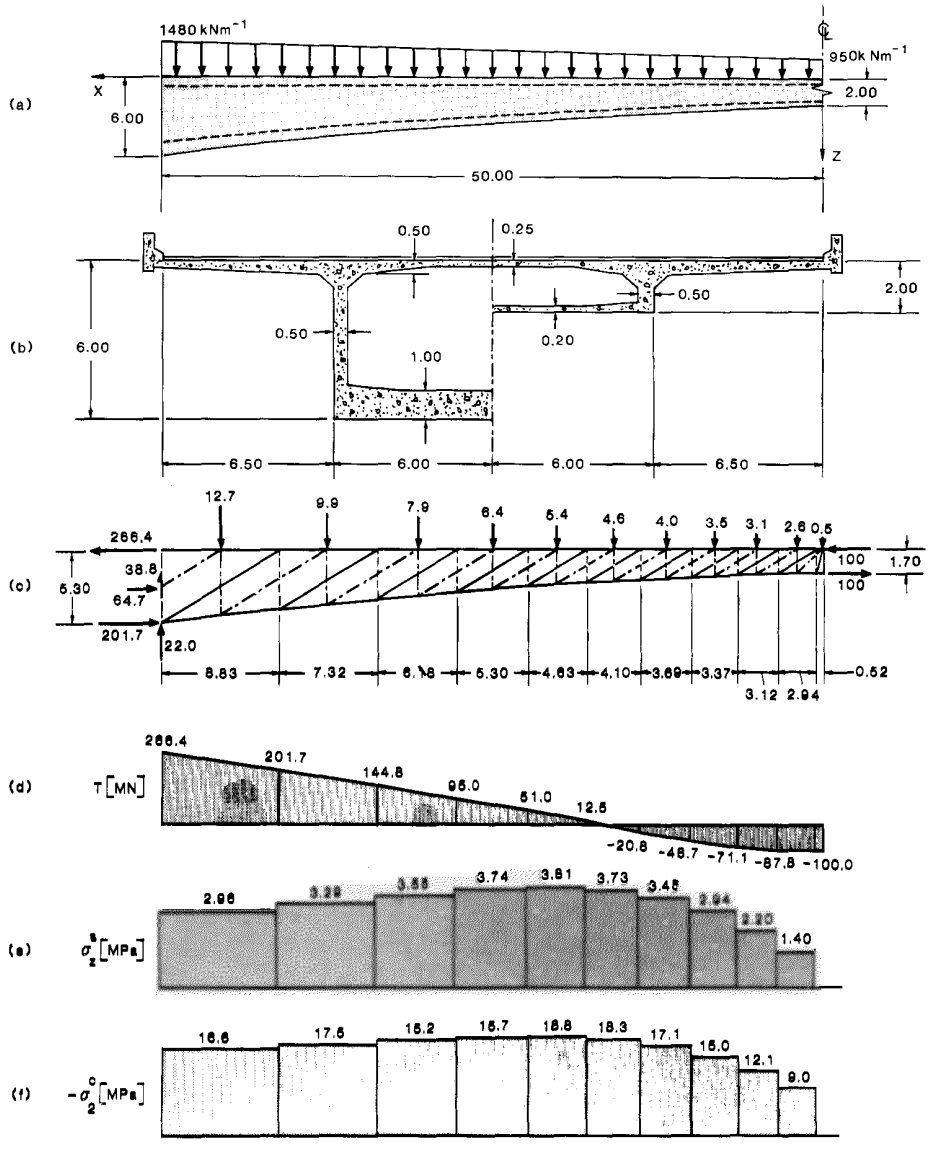

Fig. 10 — Design example 3: (a) Geometry and loading (1 m = 39.4 in., 1 kN = 0.225 kip); (b) Cross section at support (left) and at midspan (right); (c) Truss model; (d) Variation of top flange force (1 MN = 224.8 kips); (e) Required stirrup strength per unit area of web (1 MPa = 145 psi); (f) Principal compressive stresses in concrete at top of web

The truss model of Fig. 10(c) is based on an assumed inclination of the diagonals of $\tan^{-1}0.6$. At midspan a fan is used to transfer the load acting on the first 0.52 m (20.5 in.) The linearly variable ultimate load given in Fig. 10(a) is replaced by single loads acting at the centers of the 0.52-m (20.5-in.) lengths, etc. Since only their magnitudes, not their positions, coincide with those of the resultants of the actual trapezoidal load blocks, this procedure is slightly conservative.

Assuming an ultimate moment of 170MN·m (125,400 ft-kips) at midspan, the variation of the top flange force given in Fig. 10(d) results. Fig. 10(e) shows the necessary strength of the vertical stirrups per unit area of the webs. Additional stirrups are required to transfer the self-weight of the bottom flange and of the webs to the top of the webs. Fig. 10(f) gives the magnitude of the principal compressive stresses in the web concrete at the connection with the top flange.

CONCLUSIONS AND RECOMMENDATIONS

An attempt has been made to promote the application of consistent equilibrium and ultimate strength considerations to the design and detailing of reinforced concrete beams. A set of basic tools has been described. Comparisons with experiments on a shearwall coupling beam and on a deep beam have been made and three design examples have been given to illustrate the practical application of these tools.

It is proposed to determine the concrete dimensions and the dimensions, the distribution, and the details of the reinforcement by developing and drawing to scale truss models and stress fields corresponding to possible equilibrium systems of the internal forces in the concrete and in the reinforcement under ultimate loads. The stress fields consist of struts and ties, nodes, fans, and arches. Replacing fans and arches by statically equivalent struts or strut systems facilitates the devel-

opment of suitable stress fields. The necessary minimum dimensions of the struts and nodes are determined by the effective concrete compressive strength f_c. It is suggested that an average value $f_c = 0.6f'_c$ be assumed. Deviations from this value may be indicated depending on the required redistribution of the internal forces, the detailing of the reinforcement, the effect of any lateral confinement, and similar influences. A refined assessment of f_c in critical cases should be based on a consideration of the strains which are associated with the assumed stress fields.

The proposed design method is adaptable to arbitrary geometrical and loading situations. It is felt to be sufficiently elaborate but still simple and clear. Further research should focus on improving the present knowledge of its limits of applicability. In addition, there is a considerable potential for applying interactive computer programs with graphical input and output routines which could replace the traditional drawing board methods for developing truss models. Apart from ultimate strength considerations, such programs would allow investigation of the deformations in the cracked state by taking into account appropriate truss member stiffnesses. Besides, the support reactions of continuous beams and frames would be assessed more realistically than according to the normally adopted linear elastic analyses of the uncracked structures.

ACKNOWLEDGMENTS

Support from the Swiss Federal Institute of Technology, Zürich, Switzerland, the University of Toronto, and the Natural Sciences and Engineering Research Council of Canada is gratefully acknowledged.

REFERENCES

1. *IABSE Colloquim on Plasticity in Reinforced Concrete* (Copenhagen, 1979), International Association for Bridge and Structural Engineering, Zürich, V. 28, *Introductory Report,* 1978, 172 pp., and V. 29, *Final Report,* 1979, 360 pp.

2. Nielsen, M. P.; Braestrup, M. W.; Jensen, B. C.; and Bach, F., "Concrete Plasticity," *Specialpublikation,* Dansk Selskab for Bygningsstatik, Copenhagen, 1978, 129 pp.

3. Thürlimann, B.; Marti, P.; Pralong, J.; Ritz, P.; and Zimmerli, B., "Application of the Theory of Plasticity to Reinforced Concrete (Anwendung der Plastizitaetstheorie auf Stahlbeton)," Institute of Structural Engineering, ETH Zürich, 1983, 252 pp.

4. Chen, W. F., *Plasticity in Reinforced Concrete,* McGraw-Hill Book Co., New York, 1982, 474 pp.

5. "Ultimate Strength and Plastic Design of Reinforced and Prestressed Concrete Structures," Directive 162/34 concerning the Structural Design Standard SIA 162, Swiss Society of Engineers and Architects, Zürich, 1976, 14 pp.

6. *CEB-FIP Model Code for Concrete Structures,* 3rd Edition, Comité Euro-International du Béton/Fédération Internationale de la Précontrainte, Paris, 1978, 348 pp.

7. "Concrete, Reinforced and Prestressed Concrete (Beton, Stahlbeton und Spannbeton)," Structural Design Standard SIA 162, 1. Draft, Swiss Society of Engineers and Architects, Zürich, 1982, 60 pp.

8. Collins, Michael P., and Mitchell, Denis, "Shear and Torsion Design of Prestressed and Non-Prestressed Concrete Beams," *Journal,* Prestressed Concrete Institute, V. 25, No. 5, Sept.-Oct. 1980, pp. 32-100. Also, Discussion and Closure, V. 26, No. 6, Nov.-Dec. 1981, pp. 96-118.

9. Johansen, K. W., *Yield-Line Theory,* Cement and Concrete Association, London, 1962, 181 pp.

10. Hillerborg, Arne, *Strip Method of Design,* Cement and Concrete Association, Wexham Springs, 1975, 256 pp.

11. Park, Robert, and Gamble, William L., *Reinforced Concrete Slabs,* John Wiley & Sons, New York, 1980, 618 pp.

12. Mueller, P., "Plastic Analysis of Reinforced Concrete Walls and Beams (Plastische Berechnung von Stahlbetonscheiben und-balken)," *Report* No. 83, Institute of Structural Engineering, ETH Zürich, 1978, 160 pp.

13. Nielsen, M. P., "On the Strength of Reinforced Concrete Discs," *Civil Engineering and Building Construction Series* No. 70, Polytechnica Scandinavica, Stockholm, 1971, 261 pp.

14. Marti, P., "On Plastic Analysis of Reinforced Concrete (Zur plastischen Berechnung von Stahlbeton)," *Report* No. 104, Institute of Structural Engineering, ETH Zürich, 1980, 176 pp.

15. Marti, P., "Strength and Deformations of Reinforced Concrete Members Under Torsion and Combined Actions," *Bulletin d'Information* No. 146, Comité Euro-International du Béton, Paris, Jan. 1982, pp. 97-138.

16. Moersch, E., *Reinforced Concrete Construction—Theory and Application (Der Eisenbetonbau—Seine Theorie und Anwendung),* 5th Edition, K. Wittwer, Stuttgart, 1922, V. 1, Part 2, p. 112.

17. Drucker, D. C., "On Structural Concrete and the Theorems of Limit Analysis," *IABSE Proceedings,* V. 21, 1961, pp. 49-59.

18. Thürlimann, B., and Marti, P., "Plasticity in Reinforced Concrete (Plastizitaet im Stahlbeton)," *Lecture Notes,* Department of Civil Engineering, ETH Zürich, 1981.

19. Paulay, T., "The Coupling of Shear Walls," thesis, University of Canterbury, Christchurch, 1969.

20. Lee, D. D. K., "An Experimental Investigation in the Effects of Detailing on the Shear Behaviour of Deep Beams," MASc thesis, University of Toronto, 1982, 138 pp.